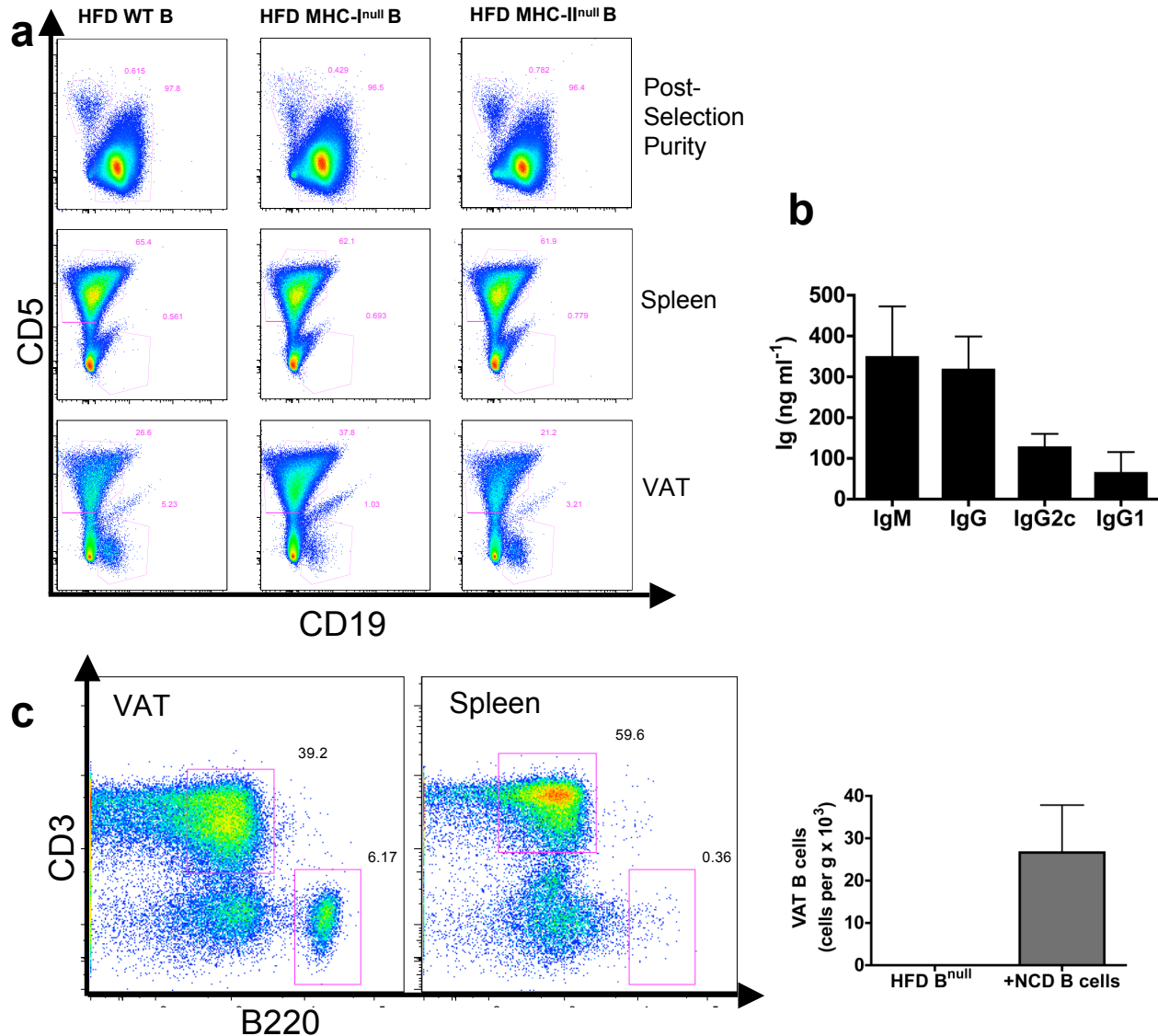
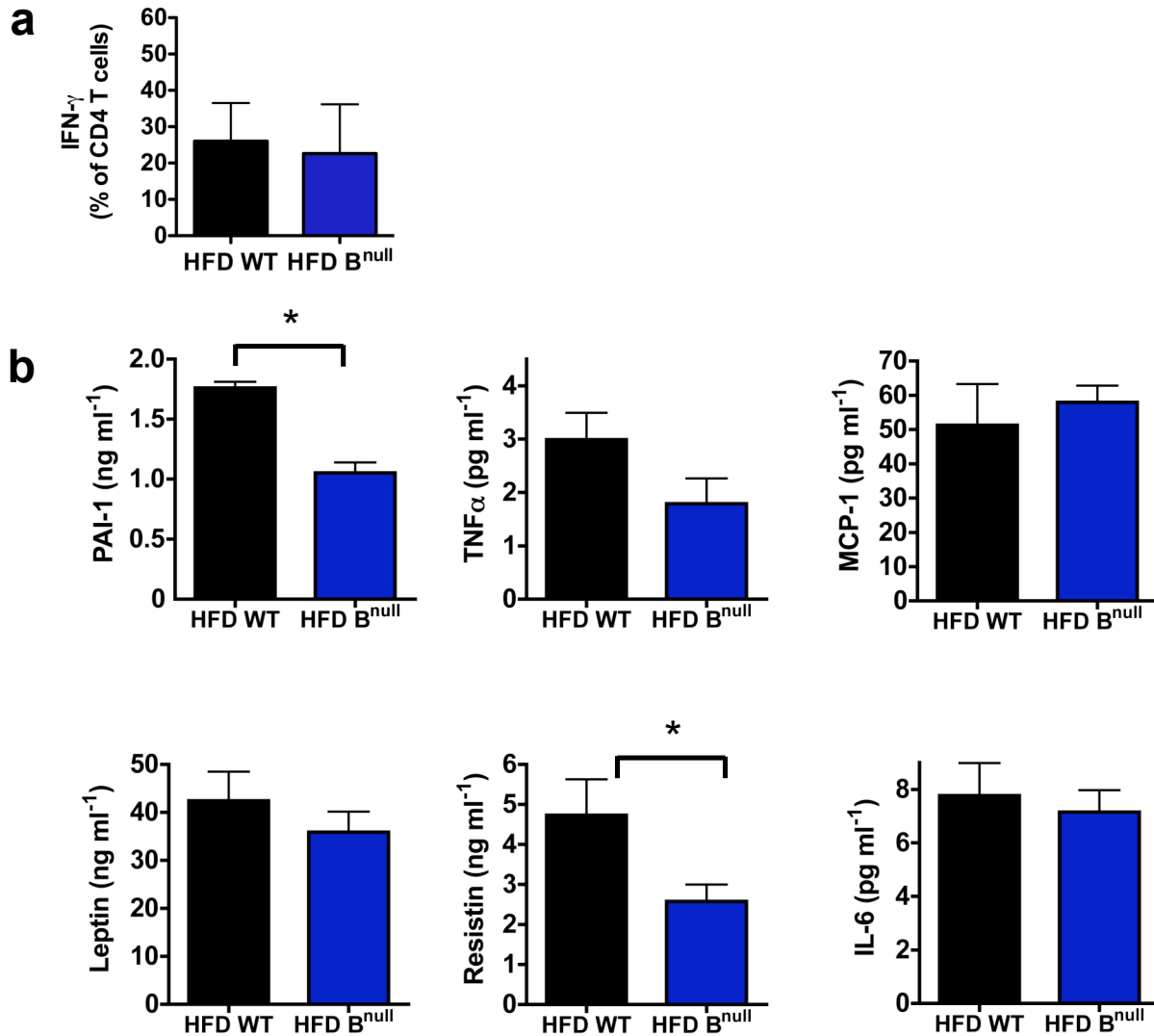


B Cells Promote Insulin Resistance through Modulation of T Cells and Production of Pathogenic IgG Antibodies

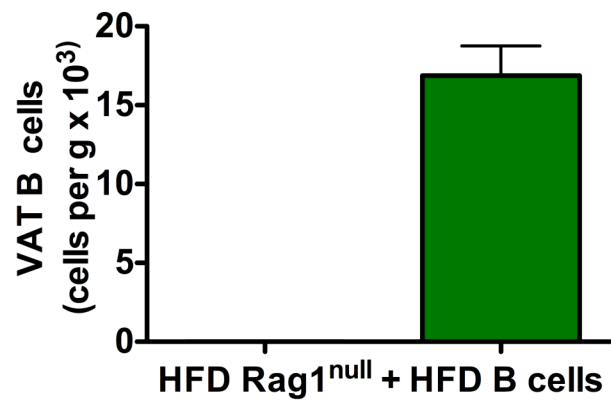
Daniel A. Winer*, Shawn Winer*, Lei Shen*, Persis P. Wadia, Jason Yantha, Geoffrey Paltser, Hubert Tsui, Ping Wu, Matthew G. Davidson, Michael N. Alonso, Hweixian Leong, Alec Glassford, Maria Caimol, Justin Kenkel, Thomas F. Tedder, Tracey McLaughlin, David B. Miklos, H.-Michael Dosch, and Edgar G. Engleman



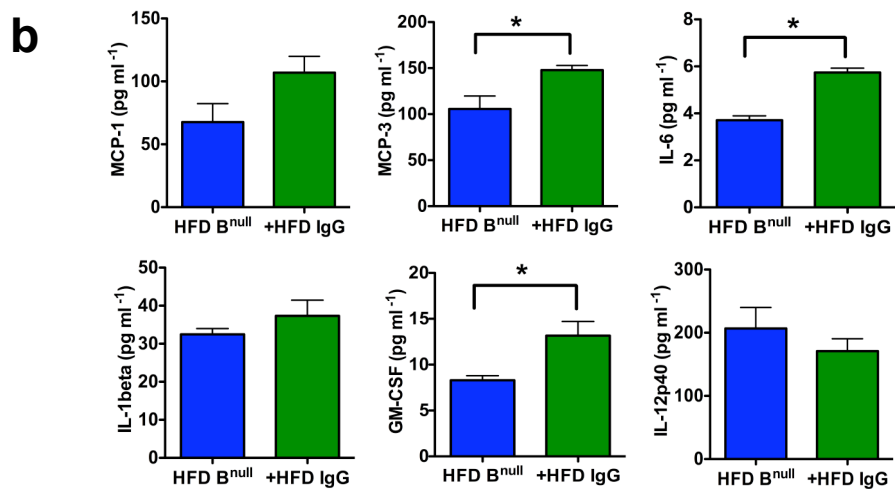
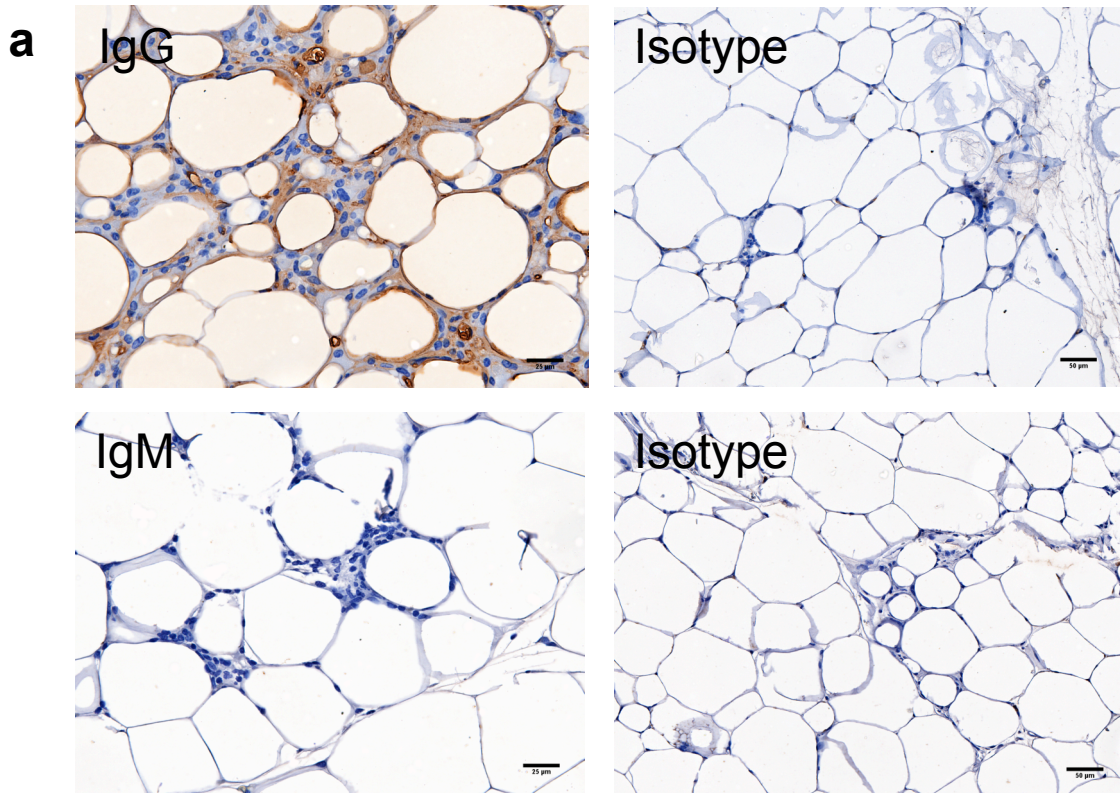
Supplementary Figure 1. B cells traffic to VAT after *i.p.* transfer. (**a**, top row) FACS plot of purified B cells isolated by negative selection from either DIO WT, MHC-I^{null} or MHC-II^{null} mice. Two weeks after *i.p.* injection into DIO B^{null} mice, CD19⁺ cells are not found in spleen (**a**, middle row) but are found in VAT (**a**, bottom row) (representative of three independent experiments). (**b**) Antibody concentrations 3 weeks after HFD B cell transfer into DIO B^{null} mice ($n = 5$). (**c**) B cell trafficking to VAT (left, right) and spleen (middle) 3 wks after *i.p.* transfer of NCD B cells (representative of 2 independent experiments).



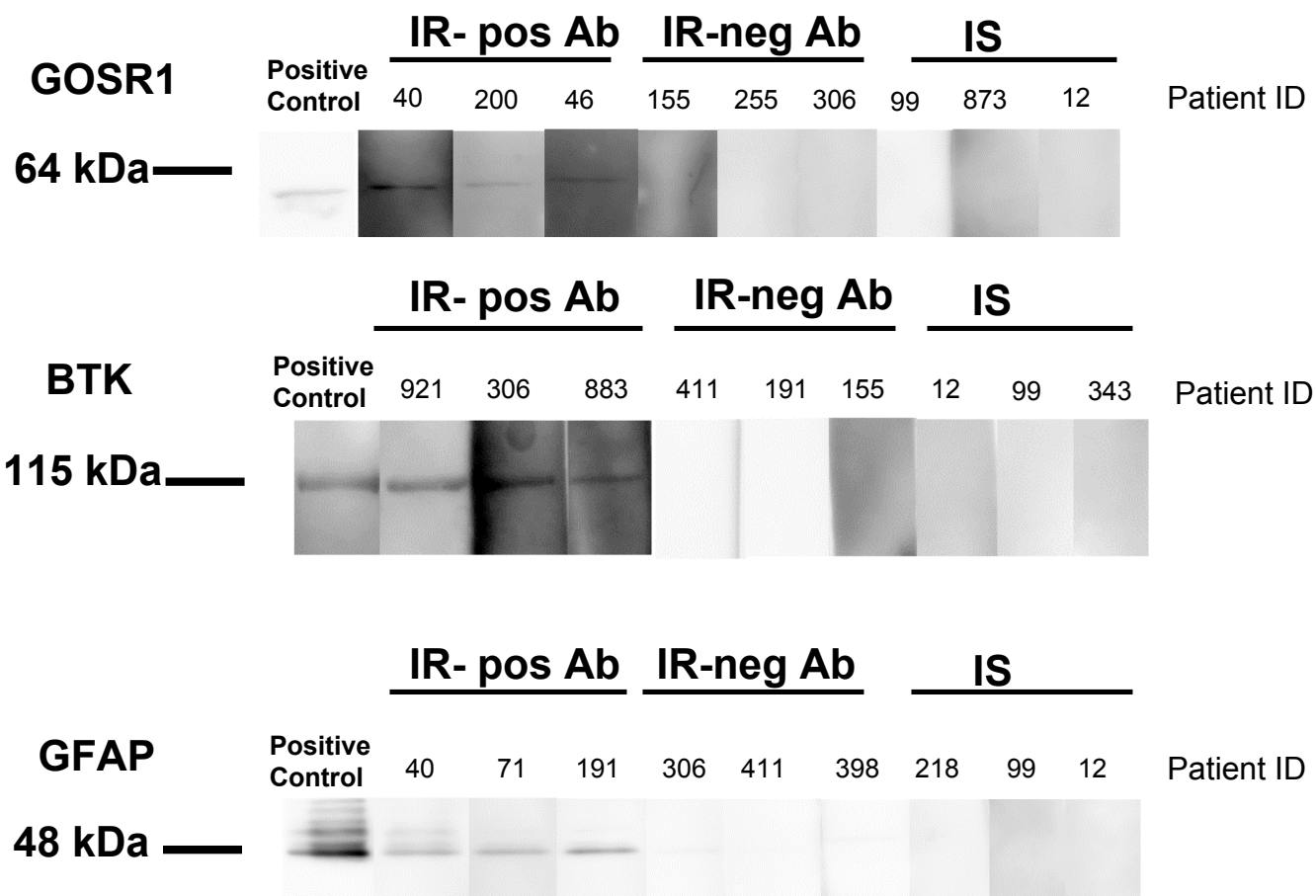
Supplementary Figure 2. Cytokine profiles in DIO B^{null} mice **(a)** Intracellular IFN- γ staining of CD4⁺ T cells isolated from VAT of 16 weeks old HFD WT and HFD B^{null} mice ($n = 3$ independent experiments, 9 mice). **(b)** Serum concentrations of obesity and insulin resistance associated adipokines and cytokines in 16 weeks old HFD WT mice compared to age matched HFD B^{null} mice. (* $P < 0.05$, $n = 5$ serum samples per group).



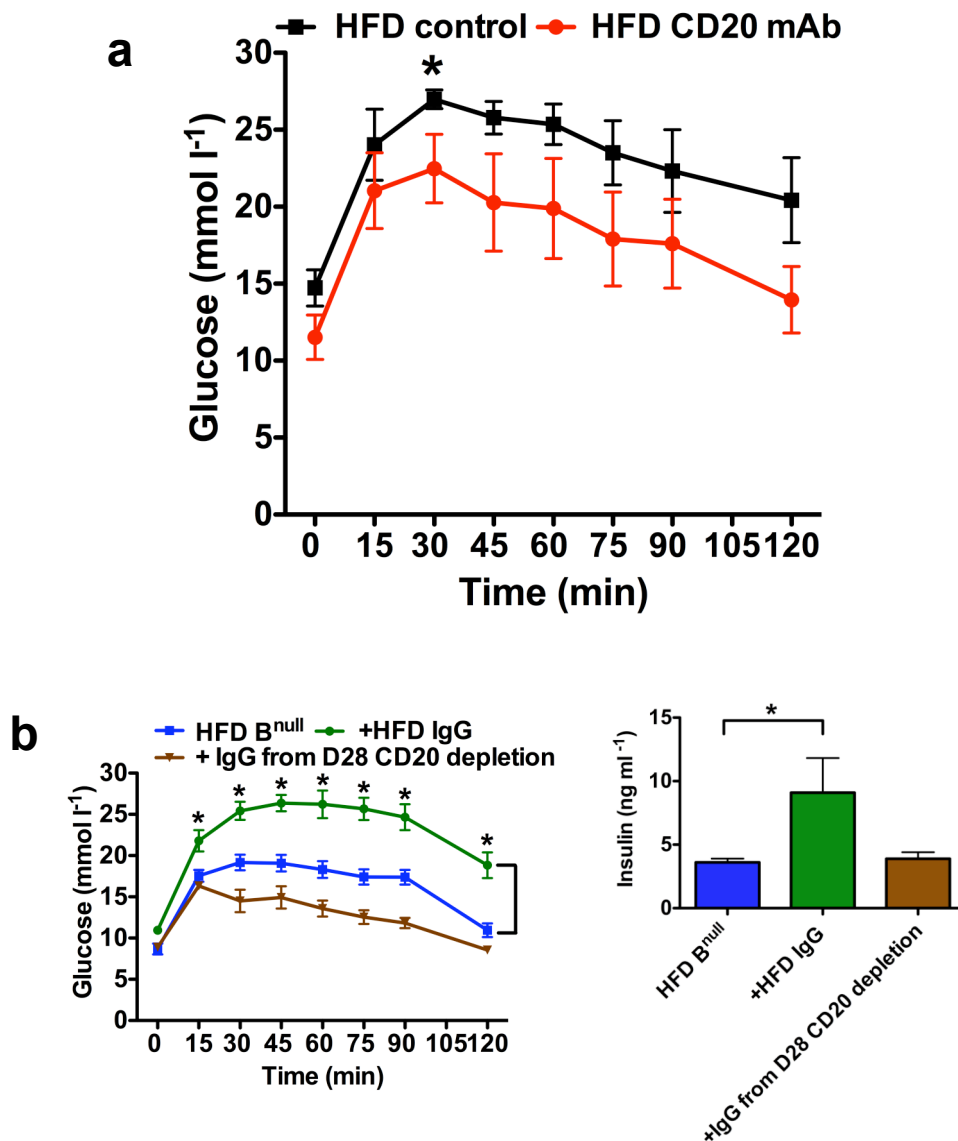
Supplementary Figure 3. B cells traffic to VAT in RAG1^{null} mice. B cell reconstitution of VAT in HFD RAG1^{null} mice 2 weeks after *i.p.* transfer of 1x10⁷ total DIO B cells (*n* = 3 mice).



Supplementary Figure 4. HFD IgG localization and effects on serum cytokines following *i.p.* transfer (a) IgG (top) and IgM (bottom) in VAT of DIO B^{null} mice one week post HFD IgG antibody transfer (scale bar 25 μm left, and 50 μm right). (b) Serum concentrations of key obesity and insulin resistance associated cytokines one week after transfer of HFD IgG relative to PBS control (**P* = 0.048 for MCP-3, **P* = 0.041 for GM-CSF; **P* = 0.0015 for IL-6, *n* = 3 serum samples per group).



Supplementary Figure 5. Validation of insulin resistant (IR) autoantibody targets in obese human subject serum. Shown are Western blots representing IR patients with higher levels of autoantibody (IR-pos Ab), no level of autoantibody (IR-neg Ab), or insulin sensitive (IS) patients which lack autoantibody against the displayed targets which represent the top 3 antigens based on human array data.



Supplementary Figure 6. Additional treatment effects of CD20 mAb in HFD mice. **(a)** GTT in HFD WT mice 40 days after receiving either CD20 mAb or control (IgG2c or PBS) ($*P < 0.05$, $n = 6$ per group). **(b)** GTT (left) and fasting insulin (right) of HFD B^{null} mice 1 week after receiving serum antibodies from CD20 mAb treated mice (+IgG from D28 CD20 depletion) or HFD IgG ($n = 5$, $*P < 0.05$).

Supplementary Table 1: Demographic and clinical characteristics of 32 BMI-matched males classified as insulin resistant or insulin sensitive (mean \pm SD) used for protoarray analysis

	IR (n=16)	IS (n=16)	P-value
Age (yrs)	55 \pm 10	54 \pm 7	0.83
Race (c/a/h/b)	11/5/0/0	15/1/0/0	0.17
BMI (kg/m ²)	31.1 \pm 2.4	31.1 \pm 2.3	0.99
Waist (cm)	109 \pm 8	107 \pm 9	0.70
SSPG (mg/dL)	238 \pm 32	87 \pm 17	<0.001
Fasting glucose (mg/dL)	105 \pm 9	98 \pm 7	0.07
Systolic BP (mmHg)	131 \pm 14	131 \pm 22	0.99
Diastolic BP (mmHg)	79 \pm 10	81 \pm 10	0.61
Total Cholesterol (mg/dL)	194 \pm 35	179 \pm 40	0.34
Triglycerides (mg/dL)*	165 \pm 106	108 \pm 62	0.12
LDL Cholesterol (mg/dL)	125 \pm 24	110 \pm 37	0.28
HDL Cholesterol (mg/dL)	39.9 \pm 6.9	48 \pm 11	0.05

Supplementary Methods

B cell purification. We mechanically dissociated spleens on 70 μ m nylon cell strainers followed by negative selection with a mouse B cell enrichment kit (Stem cell Technologies). B cell purity was >95% as determined by flow cytometry. B cells from MHC I and MHC II deficient mice show normal development, which allow for their isolation^{1,2}. IgG serum levels are decreased in beta2-microglobulin-MHC I^{null} mice primarily due to poor recycling of IgG³ and B cells from CIITA-MHC II^{null} mice show increased IL-10 production only in response to exogenous stimulation, conditions not used in our protocols pre-transfer².

Antibody ELISpot Assay. We determined the frequency of spontaneous IgM- and IgG-producing B cells in spleen using mouse IgG or IgM ELISpot^{PLUS} Kits (Mabtech). Freshly isolated splenocytes were added to ELISpot plates and incubated for 20 hours at 37 °C. Specific antibody binding spots were visualized with substrate 5-bromo-4-chloro-3-indolyl phosphate/NBT-plus (Mabtech). Developed plates were evaluated and read by ZellNet Consulting.

Flow cytometry. We stained splenocytes or fat-associated cells for 30 min with commercial antibodies to the following proteins with dilutions as recommended by the vendor. CD5-PE-Cy5 (53-7.3), CD19-PerCP-Cy5.5 (6D5), IgG-FITC (poly 4060), IgD-APC (11-26c.2a), IgM-PE (RMM-1), CD45.2-Alexa700 (104), CD21-PacBlue (7E9), CD3-PE (145-2C11), CD4-PacBlue (GK1.5), CD107a-APC (1D4B), F4/80-PerCP-Cy5.5 (BM8), CD206-FITC (MR5D3), Gr-1-APC-Cy7 (RB6-8C5), CD11b-PacBlue (M1/70), CD11c-PE-Cy7 (N418), CD1d-PerCP-Cy5.5 (1B1), and CD86-APC (GL-1) were from BioLegend. B220-PE-TR(RA3-6B2), CD8-PE-Cy5 (53-6.7), CD80-PE (16-10A1), and TNF- α -PE (MP6-XT22) were from BD Biosciences. CD23-PE-Cy7 (B3B4), and IFN- γ -APC (XMG1.2) were from eBioscience.

Purification and transfer of IgG and generation of F(ab')₂ fragments. We purified IgG from mouse serum using a Melon Gel IgG Spin Purification Kit (Pierce Biotechnology). The flow-through from the column containing IgG was dialyzed against endotoxin-free PBS and further filtered to obtain sterile antibody solution. 150 µg IgG in 200 µl endotoxin-free PBS was passively transferred to B^{null} mice via *i.p.* injections on days 1 and 3. GTT was performed at one or four weeks after IgG transfer. We generated F(ab')₂ fragments using a Pierce F(ab')₂ Preparation Kit (Thermo Scientific) according to vendor's instructions. F(ab')₂ was further purified through dialysis (50 kDa) and validated for purity by electrophoresis.

Purification and transfer of IgM. We purified IgM from serum using an IgM Purification Kit from Pierce Biotechnology. IgM containing eluate was concentrated using Amicon Ultra-15 Centrifugal Filter device (Millipore). The concentrate was dialyzed in endotoxin-free PBS and filtered to obtain sterile antibody solution which was assessed for purity by ELISA (Bethyl Laboratories). 120 µg IgM in 200 µl endotoxin-free PBS was passively transferred into B^{null} mice via *i.p.* injections on days 1 and 3. GTT was performed at one week after IgM transfer.

Human Subjects. We obtained sera from 32 age and BMI matched overweight to obese male subjects. (mean age IR: 55 ± 10, IS: 54 ± 7; mean BMI IR: 31.1 ± 2.4 kg per m²; IS: 31.1 ± 2.3 kg per m²). Insulin sensitivity was determined by a modified insulin suppression test and defined as either IR or IS based on steady-state plasma glucose (SSPG) levels falling in the top (IR) or bottom (IS) 40th percentile⁴. We excluded subjects based on the presence of major organ disease or change in physiological functioning, including heart failure, coronary artery disease, hepatic or renal disease, pregnancy, cancer, infection, recent weight gain or loss of >3 kg over 4 weeks, prior liposuction/bariatric surgery, and use of medications intended for weight loss or known to influence insulin sensitivity. Serum samples were obtained under approval by the Stanford Internal Review Board (IRB) for Human Subjects.

Human Antibody Array. We utilized ProtoArrays Version 5.0 (Invitrogen) with 1:500 diluted human sera run according to vendor's instructions. We scanned the slides using a GenePix scanner (GenePix 4000B, Molecular Devices) at a photomultiplier (PMT) gain of 60% with a laser power of 90% and a focus point of 0 μ m. The .gal file was obtained from the ProtoArray central portal on the Invitrogen website by submitting the barcode of each ProtoArray. Duplicate spot detection was highly reproducible ($R^2 = 0.96$). Data analysis was restricted to proteins with duplicate spot signal detection having coefficient of variation (CV) less than 0.5. Using Prospector Analyzer software (Invitrogen), we identified IgG targets differentially segregating with either IR or IS groups. Specifically, an IgG response required the Z score to be more than 3, coefficient of variation less than 0.5 and Chebyshev's inequality intergroup discrimination with $p < 0.05$. Chebyshev's inequality p -value is derived by testing the null hypothesis and the Z score indicating the deviation of each protein's antibody reading from its distribution mean.

Supplementary Methods References

1. Spriggs, M.K., et al. Beta 2-microglobulin-, CD8+ T-cell-deficient mice survive inoculation with high doses of vaccinia virus and exhibit altered IgG responses. *Proc Natl Acad Sci U S A* 89, 6070-6074 (1992).
2. Yee, C.S., et al. Enhanced production of IL-10 by dendritic cells deficient in CIITA. *J Immunol* 174, 1222-1229 (2005).
3. Chaudhury, C., et al. The major histocompatibility complex-related Fc receptor for IgG (FcRn) binds albumin and prolongs its lifespan. *J Exp Med* 197, 315-322 (2003).
4. McLaughlin, T., et al. Insulin resistance is associated with a modest increase in inflammation in subcutaneous adipose tissue of moderately obese women. *Diabetologia* 51, 2303-2308 (2008).